Electronic Supplementary Information

Self-healing, antibiofouling and anticorrosion properties enabled by designing polymers with dynamic covalent bonds and responsive linkages

*Jenpob Sokjorhor,[a] Tiwa Yimyai,[b] Raweewan Thiramanas,[c] and Daniel Crespy[a]**

[a] Department of Materials Science and Engineering, School of Molecular Science and Engineering, Vidyasirimedhi Institute of Science and Technology (VISTEC) Rayong 21210, Thailand

[b] Department of Chemical and Bimolecular Engineering, School of Energy Science and Engineering, Vidyasirimedhi Institute of Science and Technology (VISTEC) Rayong 21210, Thailand

[c] National Nanotechnology Center (NANOTEC), National Science and Technology Development Agency (NSTDA), Pathum Thani 12120, Thailand

Corresponding Author

* E-mail: daniel.crespy@vistec.ac.th (D. Crespy)

Table S1. Amounts of polymers and weight ratios of total disulfide bonds (S-S) of $MBTS_2MA$ units in PTM and HEDS units in PUDS compared with total weight of solvent (DMSO-d6 and $CDCl_3$).

Entry	PTM/PUDS (wt%)	PTM (mg)	PUDS (mg)	mS-S$_{(PTM+PUDS)}$/m(DMSO-d6 + $CDCl_3$) (wt%)
[PTM] + [PUDS] = constant	10	2.33	21.00	0.17
	20	4.67	18.66	0.16
	30	7.00	16.33	0.15
[PTM] = constant	10	7.00	62.99	0.51
	20	7.00	28.00	0.24
	30	7.00	16.33	0.15

Table S2. Comparison of adhesion strengths of various polyurethane coatings for anticorrosion on steel substrates.

Coating	Adhesion strength (MPa)	Ref.
Blend of PTM and PUDS	3.68 – 6.48	This work
Carbon nanotubes/TiO_2/polyurethane	1.55	1
Polyurethane with dopamine and silane pendant groups	1.70	2
Polyurethane based on acrylic polyol/hexamethylene diisocyanate	2.70	3
Polyurethane matrix Polyurethane containing micro-powdered cellulose Polyurethane containing nanocrystalline cellulose	4.58 5.18 6.51	4
Multiwalled carbon nanotube/waterborne polyurethane	5.72	5
Polyurethane Polyurethane with functionalized CeO_2 nanoparticles	7.60 9.70	6
Waterborne polyurethane containing graphene oxide	8.76	7
MXene/CeO_2 polyurethane composite	8.90	8
Polyurethane containing functionalized TiO_2 nanoparticles	11.2	9

Table S3. Corrosion current (I_{corr}), polarization resistance (R_p) and corrosion rate (CR) of steel substrates and steel substrates coated with PUDS or blends of PTM and PUDS were measured by potentiodynamic polarization in a 3.5 wt% NaCl aqueous solution.

Entry	I_{corr} (A cm^{-2})	R_p (Ω)	CR (mm year^{-1})
Bare steel	$3.36 \pm 0.11\ 10^{-6}$	$4.01 \pm 0.97\ 10^{3}$	$3.93 \pm 0.13\ 10^{-2}$
PUDS	$1.27 \pm 0.79\ 10^{-7}$	$1.52 \pm 0.82\ 10^{6}$	$1.48 \pm 0.93\ 10^{-3}$
10 wt% PTM/PUDS	$5.29 \pm 0.42\ 10^{-9}$	$1.87 \pm 0.62\ 10^{7}$	$6.18 \pm 0.49\ 10^{-5}$
20 wt% PTM/PUDS	$3.10 \pm 0.46\ 10^{-9}$	$3.51 \pm 1.96\ 10^{7}$	$3.62 \pm 0.54\ 10^{-5}$
30 wt% PTM/PUDS	$2.17 \pm 0.87\ 10^{-9}$	$4.95 \pm 2.29\ 10^{7}$	$2.54 \pm 1.02\ 10^{-5}$

Table S4. Corrosion potential (E_{corr}) and corrosion current density (I_{corr}) for the corrosion of steel coated with various polyurethane coatings immersed in a 3.5 wt% NaCl aqueous solutions.

Coating	E_{corr} (mV)	I_{corr} (A cm^{-2})	CR (mm year^{-1})	Thickness (µm)	Ref.
Blend of PTM and PUDS	-77	$2.17 \cdot 10^{-9}$	$2.54 \cdot 10^{-5}$	~ 40	This work
Waterborne polyurethane containing ZnO	-604	$7.84 \cdot 10^{-7}$	$1.00 \cdot 10^{-2}$	~ 20	10
Polyurethane containing multi-walled carbon nanotubes	n.a.	$4.39 \cdot 10^{-6}$	$5.17 \cdot 10^{-2}$	~ 63	11
Waterborne polyurethane containing montmorillonite Waterborne polyurethane Waterborne polyurethane containing functionalized Ce-montmorillonite	-564 -667 -475	$6.04 \cdot 10^{-6}$ $8.41 \cdot 10^{-6}$ $1.53 \cdot 10^{-7}$	n.a.	~ 100	12
Waterborne polyurethane containing functionalized graphene oxide and ZnO Waterborne polyurethane containing functionalized carbon black and ZnO	-482 -588	$1.90 \cdot 10^{-7}$ $9.10 \cdot 10^{-7}$	$2.00 \cdot 10^{-3}$ $1.10 \cdot 10^{-2}$	~ 20	13
Waterborne polyurethane Polyurethane containing graphene oxide Polyurethane containing functionalized graphene oxide	-320 -230 -180	$1.99 \cdot 10^{-7}$ $3.15 \cdot 10^{-8}$ $3.16 \cdot 10^{-9}$	n.a.	~ 50	14
Polyurethane containing ZnO and multiwalled carbon nanotube Polyurethane containing ZnO and reduced graphene oxide	-357 -326	$2.44 \cdot 10^{-7}$ $4.64 \cdot 10^{-8}$	$1.11 \cdot 10^{-1}$ $2.11 \cdot 10^{-2}$	~ 35	15
Polyurethane containing SiO_2 nanoparticles Polyurethane	-540 -560	$3.03 \cdot 10^{-7}$ $5.62 \cdot 10^{-7}$	$1.27 \cdot 10^{-4}$ $3.12 \cdot 10^{-4}$	~ 40	16
Polydimethylsiloxane-based polyurethane Polydimethylsiloxane-based polyurethane containing ZnO nanoparticles	-614 -487	$7.50 \cdot 10^{-8}$ $7.00 \cdot 10^{-9}$	$8.83 \cdot 10^{-3}$ $8.24 \cdot 10^{-4}$	~ 10	17
Multiwalled carbon nanotube/waterborne polyurethane	n.a.	$2.62 \cdot 10^{-9}$	$3.00 \cdot 10^{-5}$	~ 85	5
Polyurethane	-469	$6.65 \cdot 10^{-9}$	$7.72 \cdot 10^{-5}$	n.a.	18
Poly(urethane-co-pyrrole)	-91	$8.00 \cdot 10^{-9}$	n.a.	~ 10	19

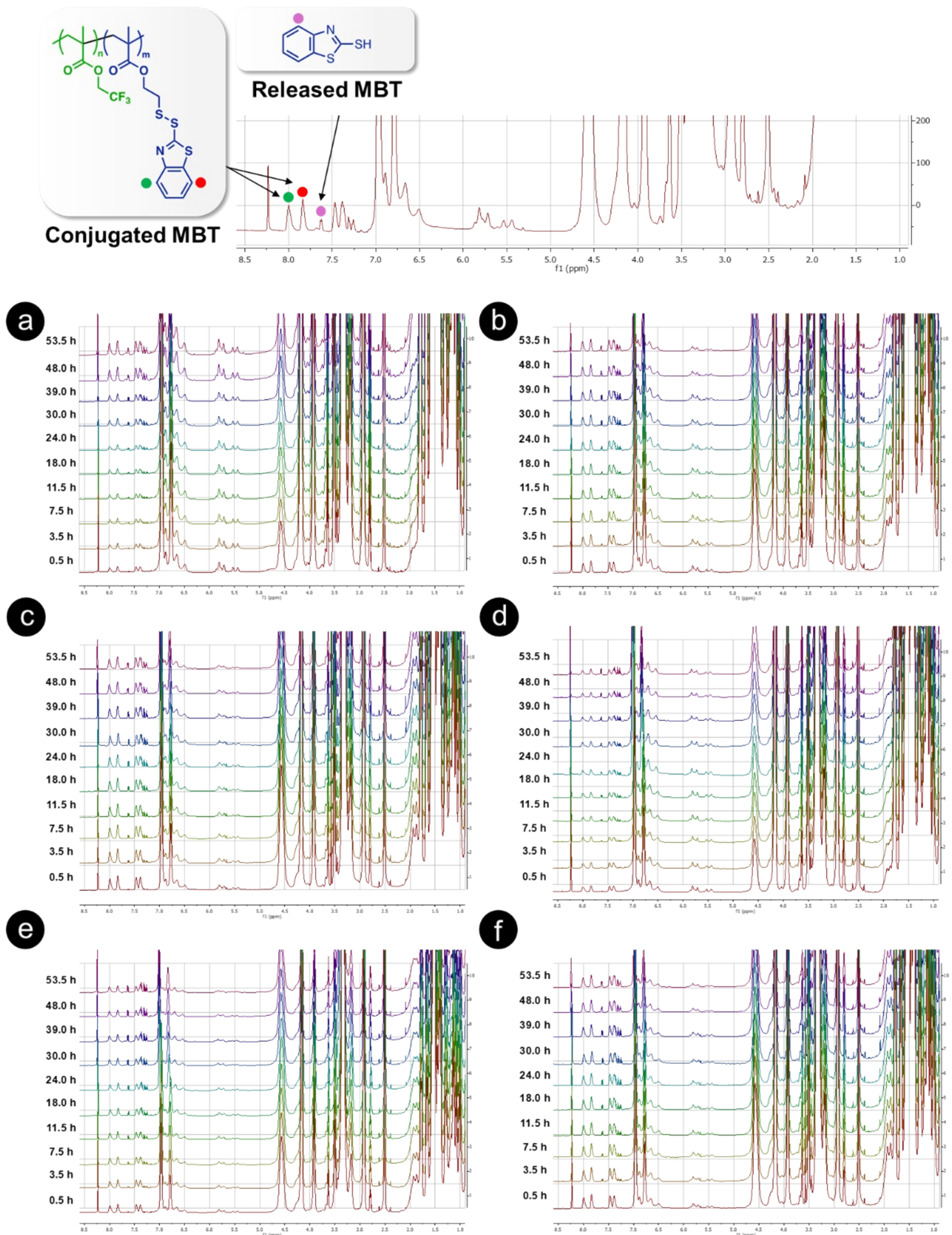

Figure S1. Temporal release of 2-mercaptobenzothiazole (MBT) from a solution of (a) 10, (b) 20, and (c) 30 wt% PTM/PUDS while keeping the concentration of polymer blends constant or from a solution of (d) 10, (e) 20, and (f) 30 wt% PTM/PUDS while keeping the concentration of PTM constant determined by ^{1}H NMR spectroscopy in a mixture of DMSO-d6 and $CDCl_3$ (80/20 v/v) at 70 °C.

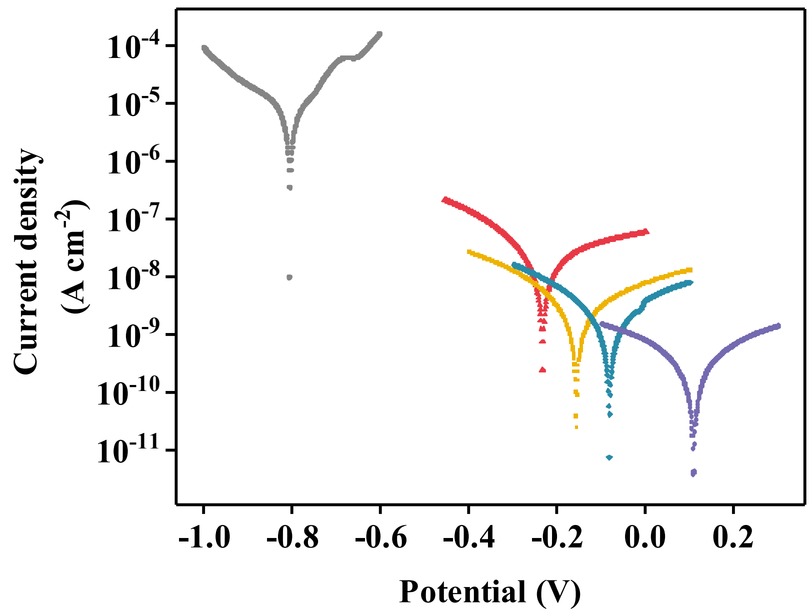

Figure S2. Potentiodynamic polarization curves of steel substrates and steel substrates coated with PUDS or blends of PTM and PUDS measured in a 3.5 wt% NaCl aqueous solution (●, bare steel; ▲, PUDS; ■, 10 wt% PTM/PUDS; ◆, 20 wt% PTM/PUDS; ⬣, 30 wt% PTM/PUDS).

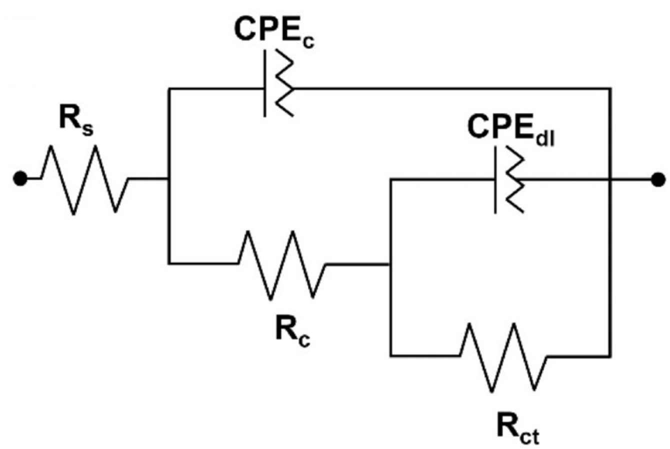

Figure S3. Equivalent circuits for modeling the data from EIS. R_c, R_{ct}, CPE_c, and CPE_{dl} are the coating resistance of the steel substrates, charge transfer resistance of the steel substrates, constant phase element of coating capacitance, and constant phase element of double-layer capacitance, respectively.

Table S5. Coating resistance (R_c), constant phase element of coating capacitance (CPE_c), charge transfer resistance (R_{ct}), and constant phase element of double-layer capacitance (CPE_{dl}) of steel substrates and steel substrates coated with PUDS or blends of PTM and PUDS were measured by electrochemical impedance spectroscopy in a 3.5 wt% NaCl aqueous solution.

Entry	R_c (Ω cm^2)	CPE_c (F cm^{-2})	R_{ct} (Ω cm^2)	CPE_{dl} (F cm^{-2})
PUDS	$2.28 \pm 0.68\ 10^5$	$1.09 \pm 0.17\ 10^{-10}$	$4.17 \pm 0.59\ 10^7$	$6.21 \pm 1.40\ 10^{-10}$
10 wt% PTM/PUDS	$2.33 \pm 0.41\ 10^5$	$0.86 \pm 0.02\ 10^{-10}$	$4.44 \pm 1.10\ 10^7$	$5.76 \pm 0.31\ 10^{-10}$
20 wt% PTM/PUDS	$2.61 \pm 0.20\ 10^5$	$0.81 \pm 0.07\ 10^{-10}$	$6.01 \pm 0.60\ 10^7$	$5.51 \pm 0.78\ 10^{-10}$
30 wt% PTM/PUDS	$2.63 \pm 0.49\ 10^5$	$0.80 \pm 0.07\ 10^{-10}$	$6.55 \pm 2.33\ 10^7$	$6.07 \pm 1.13\ 10^{-10}$

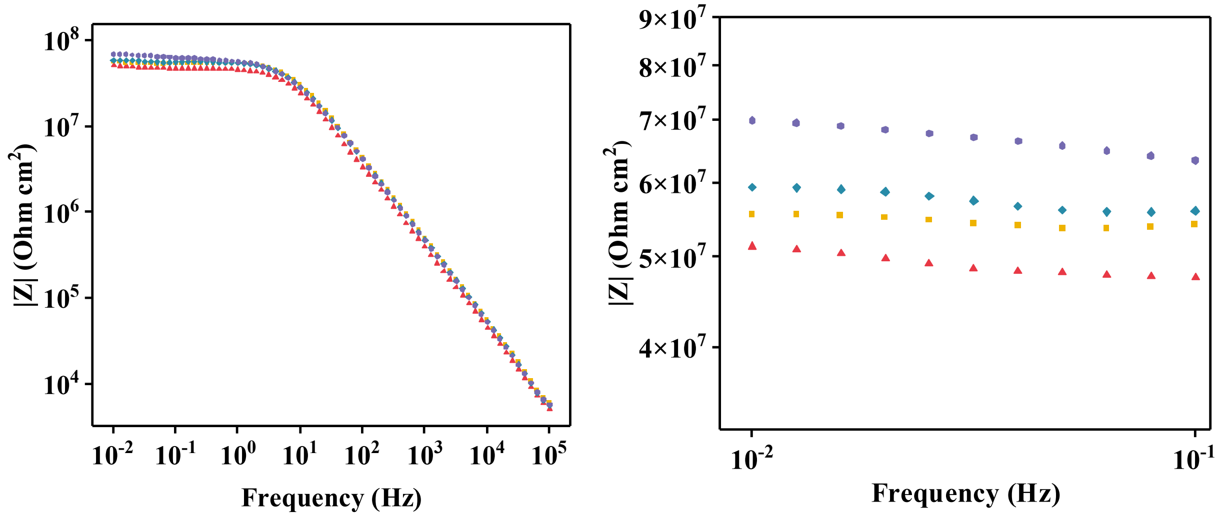

Figure S4. Bode plots of steel substrates and steel substrates coated with PUDS or blends of PTM and PUDS in a 3.5 wt% NaCl aqueous solution (▲, PUDS; ■, 10 wt% PTM/PUDS; ◆, 20 wt% PTM/PUDS; ⬢, 30 wt% PTM/PUDS).

Table S6. Impedance at 0.01 Hz ($|Z|_{0.01}$) of steel coated with various polyurethane coatings immersed in a 3.5 wt% NaCl aqueous solution.

Coating	$|Z|_{0.01}$ (Ω cm^2)	Thickness (μm)	Ref.
Blend of PTM and PUDS	$5.58 \cdot 10^7$	~ 40	This work
Polyurethane containing functionalized TiO_2 nanoparticles	~ 10^6	n.a.	9
Epoxy acrylate polyurethane	$4.49 \cdot 10^6$	n.a.	20
Waterborne polyurethane	$7.79 \cdot 10^6$	~ 40	7
Waterborne polyurethane containing graphene oxide Waterborne polyurethane containing functionalized graphene oxide	$1.15 \cdot 10^7$ $1.81 \cdot 10^7$	n.a.	21
Waterborne polyurethane Waterborne polyurethane s containing graphene oxide	$1.52 \cdot 10^7$ $6.95 \cdot 10^7$	~ 55	22
Waterborne polyurethane Waterborne polyurethane containing Ce-montmorillonite	$1.74 \cdot 10^7$ $4.10 \cdot 10^8$	~ 100	12
Polyurethane containing ZnO and multiwalled carbon nanotube	$5.68 \cdot 10^8$	~ 35	15

Table S7. Comparison of the self-healing efficiency of various polyurethane coatings for anticorrosion.

Coating	Healing condition		Measured value	Healing efficiency (%)	Thickness (μm)	Ref.
	T **(°C)**	***t*** **(h)**				
Blend of PTM and PUDS	70	48	integrals of Bode plots from $10^{-2} – 10^5$ Hz	~ 95	~ 40	This work
Polyurethane with dopamine and silane pendant groups	25	24	tensile strength	~ 64	~ 500	2
Polyurethane containing microcapsules loaded with an inhibitor	25	2	polarization resistance	~ 77	~ 300	23
Polyurethane with phenanthroline side chains	25	1.5	tensile strength	~ 88	~ 80	24
Polyurethane with functionalized CeO_2 nanoparticles	120	2	tensile strength	~ 90	~ 500	6

Table S7. Comparison of the self-healing efficiency of various polyurethane coatings for anticorrosion (Continuous).

Coating	Healing condition		Measured value	Healing efficiency (%)	Thickness (μm)	Ref.
	T (°C)	*t* (h)				
Waterborne polyurethane containing functionalized graphene oxide	125	(5 min)	impedance modulus at 0.01 Hz	~ 91	n.a.	25
Polyurethane containing functionalized silica nanoparticles	80	12	tensile strength	~ 95	n.a.	26
Polyurethane containing graphene oxide microcapsules with linseed oil	25	(15 days)	crack width	~ 100	~ 500	27

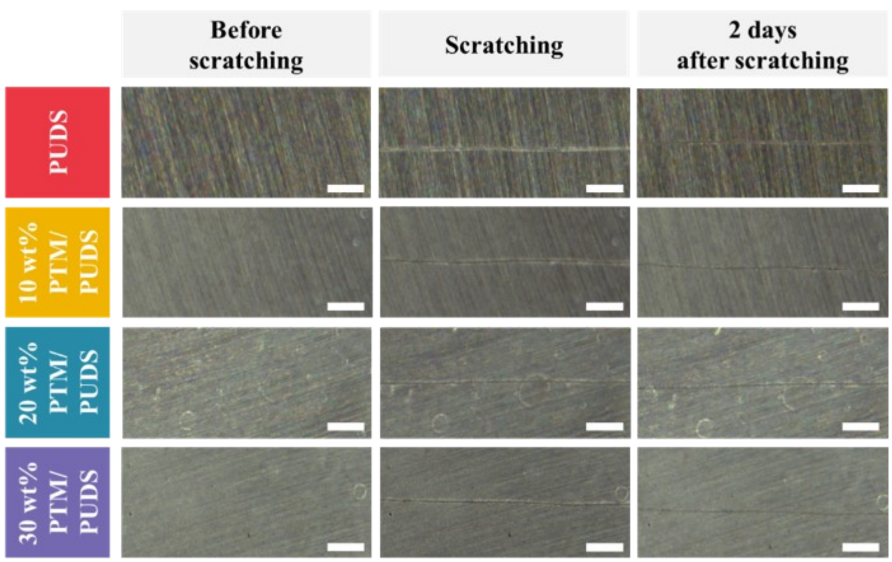

Figure S5. Photographs of steel substrates coated with PUDS or blends of PTM and PUDS after scratching (length = 5.0 mm, width = 0.4 mm) by a razor blade and healing at 70 °C for 2 days. Scale bars represent 1 mm.

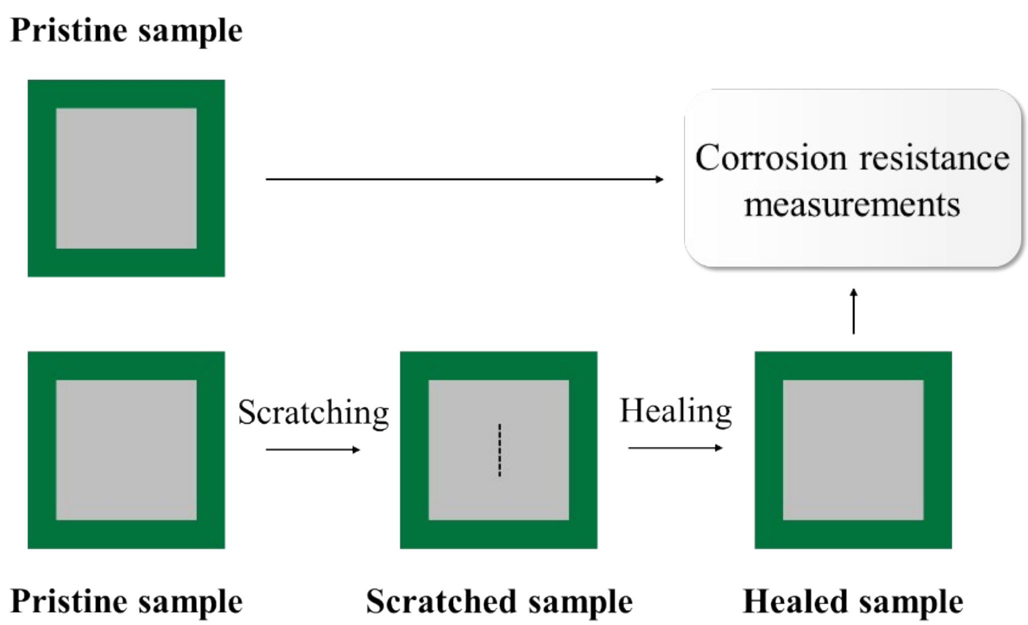

Figure S6. Schematic showing the preparation of pristine samples and scratched samples after healing at 70 °C for 2 days (length of scratch = 5.0 mm, width = 0.4 mm) for corrosion resistance measurement.

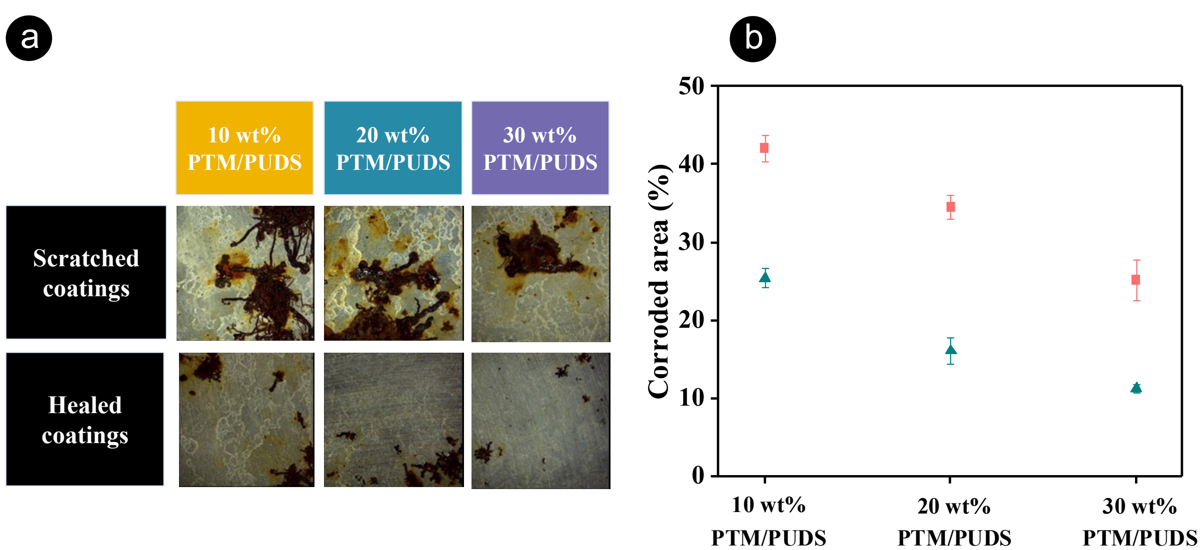

Figure S7. a) Photographs and b) calculated corroded areas of scratched (■) /healed (▲) coatings with 10, 20, and 30 wt% PTM/PUDS on steel substrates (thickness ~ 40 μm) after 48 h in a salt spray test at 35 °C.

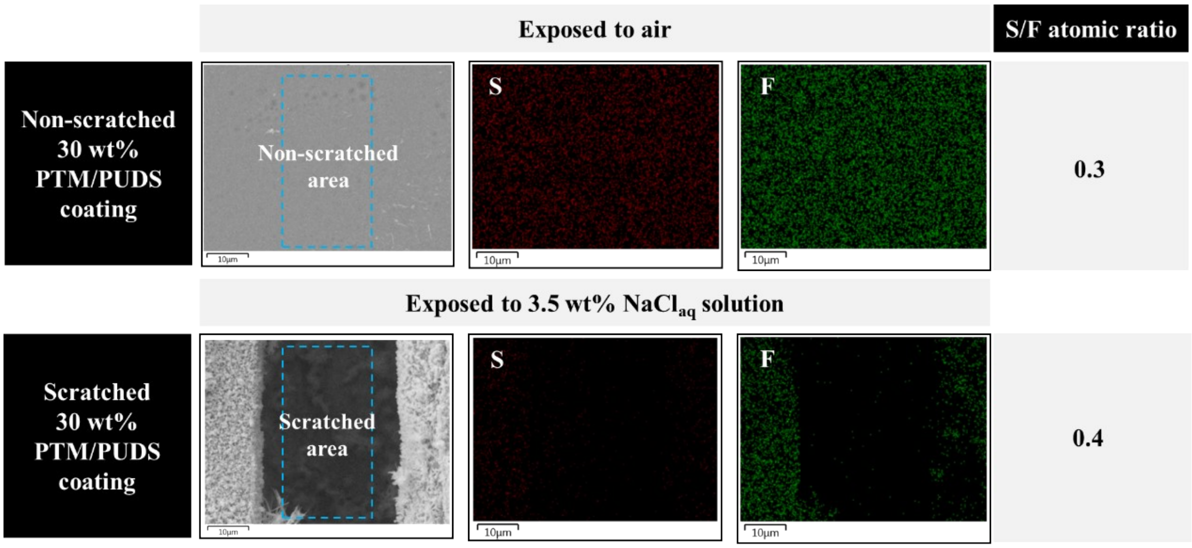

Figure S8. Energy-dispersive X-ray spectroscopy elemental mapping images and S/F atomic ratios of non-scratched and scratched 30 wt% PTM/PUDS coatings on steel substrates after exposure to 100 μL of 3.5 wt% NaCl aqueous solution after 24 h at 25 °C.

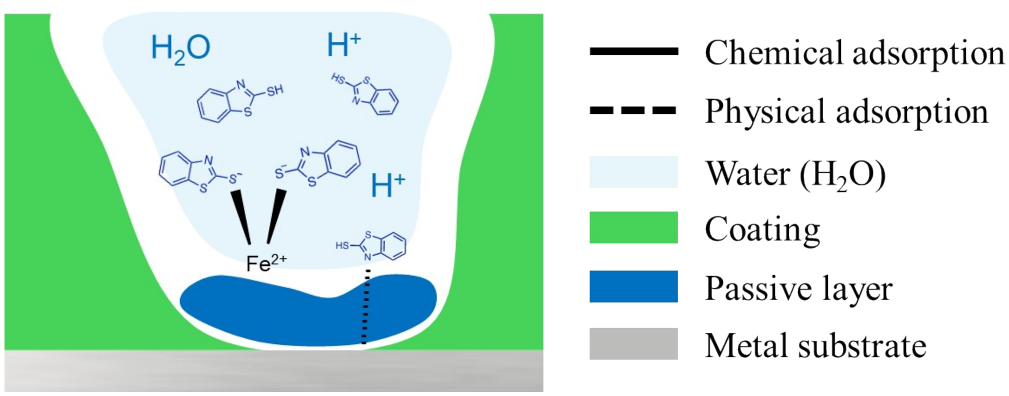

Figure S9. Schematic showing the mechanism of inhibiting corrosion reactions via the formation of passive layers.

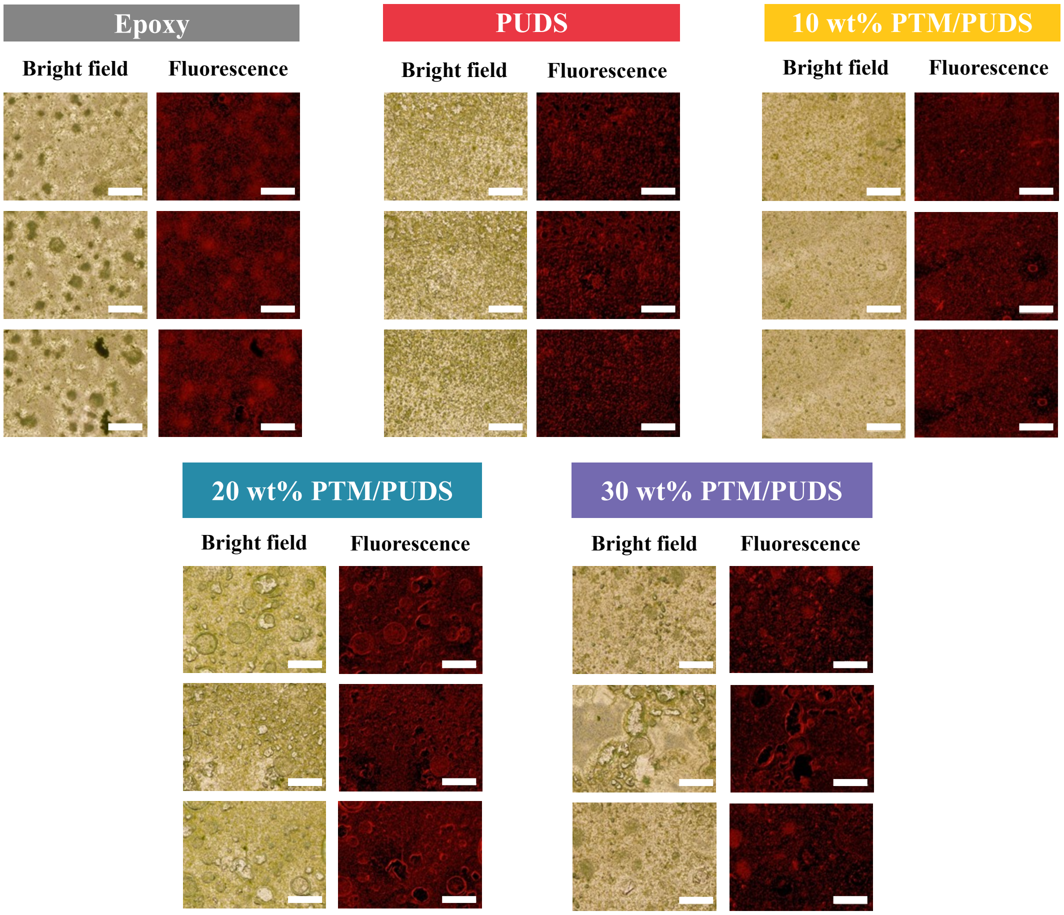

Figure S10. Photographs of coatings of epoxy, PUDS, or blends of PTM and PUDS on glass substrates taken with a bright field and fluorescence microscope after immersion for 57 days at 28 °C in a solution containing the unicellular microalgae, *Chlorella ellipsoidea.*

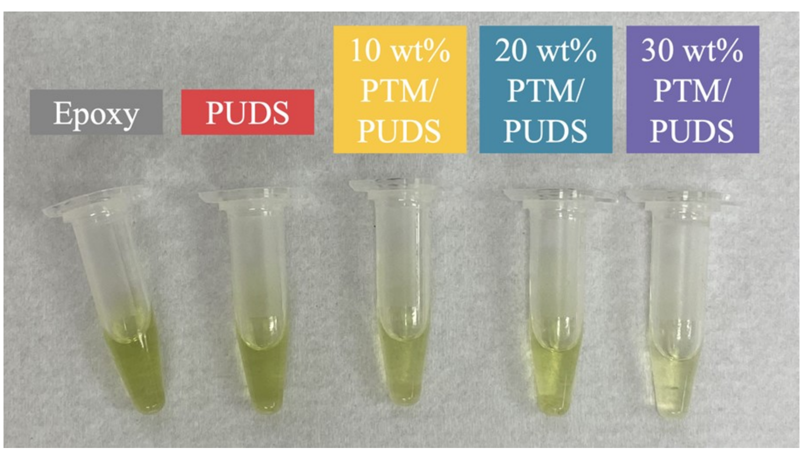

Figure S11. Photographs of DMF solutions used for extracting chlorophyll from coatings of epoxy, PUDS, and blends of PTM and PUDS on glass substrates.

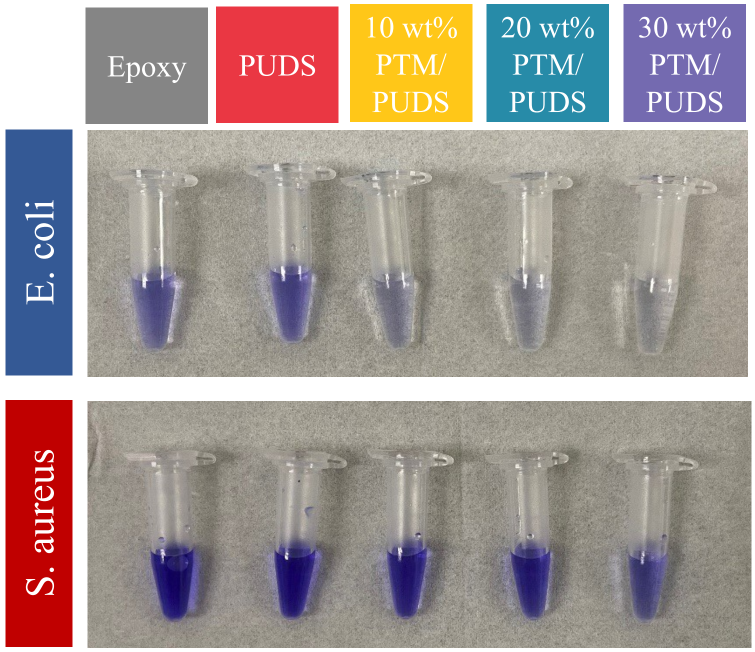

Figure S12. Photographs of crystal violet solutions used for extracting bacterial, *Escherichia coli (E. coli)* and *Staphylococcus aureus (S. aureus)*, from coatings of epoxy, PUDS, and blends of PTM and PUDS on glass substrates.

References

1. Q. X. Nguyen, T. T. Nguyen, N. M. Pham, T. T. Khong, T. M. Cao and V. V. Pham, *Prog. Org. Coat.*, 2022, **167**, 106838.
2. P. Hu, R. Xie, Q. Xie, C. Ma and G. Zhang, *J. Chem. Eng.*, 2022, **449**, 137875.
3. E. Abil and R. Arefinia, *Prog. Org. Coat.*, 2022, **172**, 107067.
4. M. Abd El-Fattah, A. M. A. Hasan, M. Keshawy, A. M. El Saeed and O. M. Aboelenien, *Carbohydr. Polym.*, 2018, **183**, 311-318.
5. F. Wang, J. Ci and J. Fan, *Polymers*, 2022, **14**.
6. H. Wang, J. Xu, X. Du, Z. Du, X. Cheng and H. Wang, *Compos. B. Eng.*, 2021, **225**, 109273.
7. Z. Zhao, L. Guo, L. Feng, H. Lu, Y. Xu, J. Wang, B. Xiang and X. Zou, *Eur. Polym. J.*, 2019, **120**, 109249.
8. H. Wang, J. Xu, X. Du, H. Wang, X. Cheng and Z. Du, *Prog. Org. Coat.*, 2022, **164**, 106672.
9. S. S. Chandraraj and J. R. Xavier, *J. Mater. Sci.*, 2022, **57**, 13362-13384.
10. G. Christopher, M. A. Kulandainathan and G. Harichandran, *Prog. Org. Coat.*, 2016, **99**, 91-102.
11. F. Wang, L. Feng and G. Li, *Polymers*, 2018, **10**.
12. S. Li, S. Wang, X. Du, H. Wang, X. Cheng and Z. Du, *Prog. Org. Coat.*, 2022, **163**, 106613.
13. G. Christopher, M. Anbu Kulandainathan and G. Harichandran, *Prog. Org. Coat.*, 2015, **89**, 199-211.
14. A. Mohammadi, M. Barikani, A. H. Doctorsafaei, A. P. Isfahani, E. Shams and B. Ghalei, *J. Chem. Eng.*, 2018, **349**, 466-480.
15. K. Rajitha, K. N. S. Mohana, M. B. Hegde, S. R. Nayak and N. K. Swamy, *FlatChem*, 2020, **24**, 100208.
16. J. Verma, A. Gupta and D. Kumar, *Prog. Org. Coat.*, 2022, **163**, 106661.
17. B. John, P. R. Rajimol, T. P. D. Rajan and S. K. Sahoo, *Surf. Coat. Technol.*, 2022, **451**.
18. T. Ghosh and N. Karak, *Prog. Org. Coat.*, 2020, **139**, 105472.
19. R. Gharibi, M. Yousefi and H. Yeganeh, *Prog. Org. Coat.*, 2013, **76**, 1454-1464.
20. Y. Ahmadi and S. Ahmad, *Prog. Org. Coat.*, 2019, **127**, 168-180.
21. F. Zhang, W. Liu, C. Liu, S. Wang, H. Shi, L. Liang and K. Pi, *Colloids Surf. A: Physicochem. Eng. Asp.*, 2021, **617**, 126390.
22. F. Zhang, S. Wang, W. Liu, H. Shi, L. Liang, C. Liu, K. Pi, W. Zhang and J. Zeng, *Colloids Surf. A: Physicochem. Eng. Asp.*, 2022, **640**, 127718.
23. W. Fan, Y. Zhang, W. Li, W. Wang, X. Zhao and L. Song, *J. Chem. Eng.*, 2019, **368**, 1033-1044.
24. C. Liu, H. Wu, Y. Qiang, H. Zhao and L. Wang, *Corros. Sci.*, 2021, **184**, 109355.
25. J. Xu, F. Gao, H. Wang, R. Dai, S. Dong and H. Wang, *Prog. Org. Coat.*, 2023, **174**, 107244.
26. H. Wang, J. Xu, H. Wang, X. Cheng, S. Wang and Z. Du, *Prog. Org. Coat.*, 2022, **167**, 106837.
27. J. Li, Q. Feng, J. Cui, Q. Yuan, H. Qiu, S. Gao and J. Yang, *Compos. Sci. Technol.*, 2017, **151**, 282-290.